Reactivity of a New Aryl Cycloplatinated(II) Complex Containing Rollover 2,2´-Bipyridine *N*-Oxide toward a Series of Diphosphine Ligands

Hamid R. Shahsavari,[a] Reza Babadi Aghakhanpour,[a] Mojdeh Hossein-Abadi,[a] Reza Kia,[b]* Mohammad Reza Halvagar[c] and Paul R. Raithby[d]*

[a]Department of Chemistry, Institute for Advanced Studies in Basic Sciences (IASBS), Yousef Sobouti Blvd., Zanjan 45137-66731, Iran.

[b]Chemistry Department, Sharif University of Technology, P.O. Box 11155-3516, Tehran, Iran.

[c]Chemistry & Chemical Engineering Research Center of Iran, Tehran,14968-13151, Iran.

[d]Department of Chemistry, University of Bath, Claverton Down, BA2 7AY, Bath, UK.

Email: shahsavari@iasbs.ac.ir (H.R.S.); rkia@sharif.edu (R.K.).

Abstract

Reaction of the electron-rich complex *cis*-[Pt(*p*-Me-C_6H_4)$_2$(SMe_2)$_2$] with 2,2´-bipyridine *N*-oxide, O-bpy, occurred by rollover cyclometalation to afford complex [Pt(O-bpy)(*p*-Me-C_6H_4)(SMe_2)], **1**. The obtained complex was characterized through NMR spectroscopy and its solid state structure was determined by the single crystal X-ray diffraction method. The reaction of **1** with seven diphosphine ligands, 1,1-bis(diphenylphosphino)methane (dppm), 1,2-bis(diphenylphosphino)ethane (dppe), 1,3-bis(diphenylphosphino)propane (dppp), 1,4-bis(diphenylphosphino)butane (dppb), N,N-bis(diphenylphosphino)amine (dppa), 1,2-bis(diphenylphosphino)benzene (dppbz) and 1,1'-bis(diphenylphosphino)ferrocene (dppf), in different molar ratio (1:1 or 1:0.5; **1**:diphosphines) was studied. In accordance with the reaction conditions the analogous mononuclear or binuclear diphosphine cycloplatinated complexes were yielded. The diphosphines behave as a monodentate (dppm, dppa), a bridging (dppm, dppa, dppe, dppp, dppb, dppf) or a chelated (dppe, dppp, dppbz) ligand. These behaviors depended on the bite angle of the diphosphine ligands, flexibility or rigidity of alkyl and aromatic backbone between two phosphine groups. All diphosphine platinum complexes were characterized by NMR and the crystal structures of some complexes solved by X-ray diffraction.

Introduction

Mono and biaryl Pt(II) complexes containing chelating and labile solvent ligands reportedly have shown to be participated in many reactions such as insertion into Pt-C(Aryl) bond,[1, 2] oxidative addition,[3, 4] C-H activation[5] and transmetalation of the aryl ligand.[6] In this context, some of various C^N cycloplatinated(II) complexes with aryl ligands (*p*-tolyl, *p*-anisole, phenyl) and their reactions have been reported in the literature.[7-12] To the best of our knowledge, the presence of aryl groups as ancillary ligands in the rollover cycloplatinated(II) complexes is very scarce in the published resources.[13] In this way, thermal rearrangement of the complex $[Pt(bpy)(Ar)_2]$ (bpy = 2,2′-bipyridine, Ar = C_6H_5, *p*-^{t}Bu-C_6H_4 and *p*-CF_3-C_6H_4) results in the formation of three-coordinated monoaryl [Pt(C^N)(Ar)] intermediates *via* rollover cycloplatination process.[14] Recently, cycloplatinated(II) complexes comprising a special kind of aryl ligand named pentafluorophenyl (C_6F_5) revealed strong luminescence at room temperature.[15-18] It is worthy to note that the presence of aryl-type ancillary ligands in the structure of emissive cycloplatinated(II) complexes helps extending the π-conjugation system in such molecules.

It has been proved that the reactions of *N*-oxide derivatives of 2,2′-bipyridine (O-bpy) and 1,10-phenantroline (O-phen) with dimethylplatinum(II) complex *cis,cis*-$[Pt_2Me_4(\mu\text{-}SMe_2)_2]$ give the corresponding complexes with chelated ligands having the general formula of $[Pt(N^O)(Me)_2]$ (see scheme 1).[19] O-bpy can potentially be a C^N cyclometalated ligand through a rotation along the bond between the rings (rollover cyclometalation) while the O-phen is not able to perform such rotation due to its structural rigidity. Rollover cyclometalation in $[Pt(N^O)(Me)_2]$ (N^O = O-bpy) concomitant with the addition of SMe_2 leads to formation of $[Pt(C^N)(Me)(SMe_2)]$ (C^N = rollover O-bpy). There are some reports on replacement of SMe_2 in $[Pt(C^N)(Me)(SMe_2)]$ by different neutral ligands.[19-25]

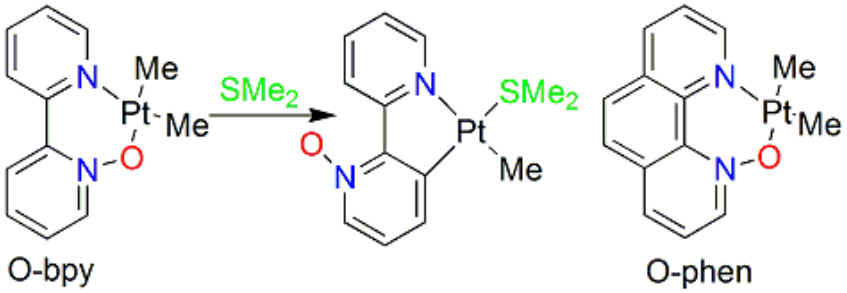

Scheme 1. Binding modes of O-bpy and O-phen chelating ligands.

On the basis of our previous experiences in chemistry of cycloplatinated(II) compounds,[20-23, 26-32] herein, we report the synthesis and characterization of a new cycloplatinated(II) precursor complex including 2,2′-bipyridine *N*-oxide (O-bpy, C^N chelate), *p*-Me-C_6H_4 and labile SMe_2 ligands ([Pt(O-bpy)(*p*-Me-C_6H_4)(SMe_2)], **1**). In the following, the reactivity of this complex toward a wide range of diphosphine ligands was investigated in order to study the different behaviors of diphosphines against the cycloplatinated(II) complex. Such different behaviors are logically due to that the steric and electronic properties of diphosphine ligands are notably controlled by their backbones. Figure 1 shows three different possible modes of binding for diphosphines in cycloplatinated(II) complexes.[8, 9, 11, 33-44]

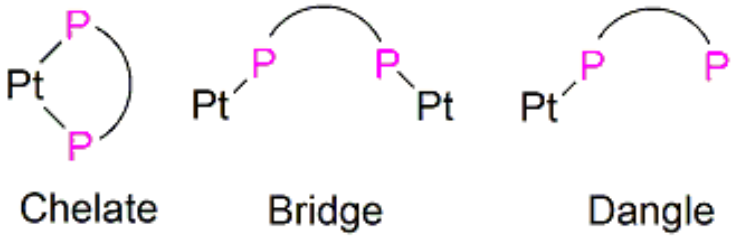

Figure 1. Different binding modes for diphosphine ligands in cycloplatinated(II) complexes.

Experimental

General Procedures and Materials

All the reactions were carried out in the common solvents and all the solvents were purified and dried according to standard procedures.[45] The microanalyses were performed using a vario EL CHNS elemental analyzer and also all the melting point values were measured by a Buchi 510. Multinuclear (^{1}H, ^{1}H{^{195}Pt}, ^{13}C{^{1}H}, ^{31}P{^{1}H}, ^{195}Pt) NMR spectra together with two dimensional NMR spectra (COSY, HSQC and NOESY) and DEPT 135° technique were recorded on a Bruker Avance DPX 400 MHz spectrometer at 298 K. All chemical shifts are reported in ppm (part per million) relative to their corresponding external standards ($SiMe_4$ for ^{1}H and ^{13}C, 85% H_3PO_4 for ^{31}P and Na_2PtCl_6 for ^{195}Pt) and also all the coupling constants (*J* values) are given in Hz. All NMR spectra are shown in Supporting Information while the corresponding numerical data are listed in Experimental Section. 2,2′-Bipyridine *N*-oxide (O-bpy), 1,1-bis(diphenylphosphino)methane (dppm), 1,2-bis(diphenylphosphino)ethane (dppe),

1,3-bis(diphenylphosphino)propane (dppp), 1,4-bis(diphenylphosphino)butane (dppb), N,N-bis(diphenylphosphino)amine (dppa), 1,2-bis(diphenylphosphino)benzene (dppbz) and 1,1'-bis(diphenylphosphino)ferrocene (dppf) were purchased from commercial resources. *cis*-[Pt(*p*-Me-C_6H_4)$_2$(SMe_2)$_2$][46] was synthesized according to the previous report. The NMR labeling is shown in Figure 2 for clarifying the chemical shift assignments.

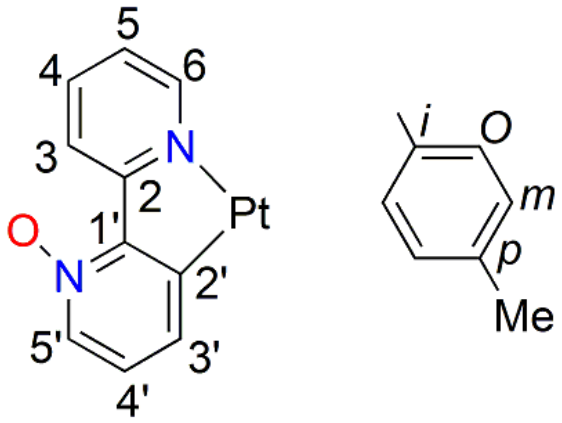

Figure 2. NMR labeling for the chemical shift assignments.

[Pt(O-bpy)(*p*-Me-C_6H_4)(SMe_2)], 1. To a solution of *cis*-[Pt(*p*-Me-C_6H_4)$_2$(SMe_2)$_2$] (500 mg, 1 mmol) in acetone (10 mL), 2,2′-bipyridine *N*-oxide (172 mg, 1 mmol) was added. Then, the reaction mixture was refluxed at 60 °C for 6 hours. The initial red color of the solution gradually became yellow and concurrently, a yellow precipitate appeared in the solution. The yellow precipitate was filtered, washed with *n*-pentane (3×3 mL) and dried under air atmosphere. Yield: 71%; m.p. = decomposed at 228 °C. Elem. Anal. Calcd. for $C_{19}H_{20}N_2OPtS$ (519.52) C, 43.93; H, 3.88; N, 5.39; S, 6.17. Found: C, 43.86; H, 3.91; N, 5.47; S, 6.21. NMR data in CD_2Cl_2: δ(^{1}H) = 2.12 [s, 6H, $^3J_{PtH}$ = 25.9 Hz, SMe_2], 2.23 [s, 3H, Me of *p*-Me-C_6H_4], 6.72 [d, 1H, $^3J_{HH}$ = 7.2 Hz, $^3J_{PtH}$ = 73.4 Hz, H$^{3'}$], 6.82 [t, 1H, $^3J_{HH}$ = 7.2 Hz, $^4J_{PtH}$ = 24.1 Hz, H$^{4'}$], 6.89 [d, 2H, $^3J_{HH}$ = 7.8 Hz, H^m of *p*-Me-C_6H_4], 7.28 [d, 2H, $^3J_{HH}$ = 7.8 Hz, $^3J_{PtH}$ = 58.9 Hz, H^o of *p*-Me-C_6H_4], 7.46 [dd, 1H, $^3J_{HH}$ = 7.3 Hz, $^3J_{HH}$ = 5.4 Hz, H^5], 7.89 [dd, 1H, $^3J_{HH}$ = 6.2 Hz, $^4J_{HH}$ = 0.9 Hz, H$^{5'}$], 8.04 [td, 1H, $^3J_{HH}$ = 8.1 Hz, $^4J_{HH}$ = 1.6 Hz, H^4], 9.03 [dd, 1H, $^3J_{HH}$ = 5.4 Hz, $^4J_{HH}$ = 1.1 Hz, $^3J_{PtH}$ = 21.4 Hz, H^6], 9.82 [d, 1H, $^3J_{HH}$ = 8.3 Hz, H^3]; δ(^{13}C in acetone-d_6) = 20.7 [s, 2C, SMe_2], 21.0 [s, 1C, Me of *p*-Me-C_6H_4], 124.8 [s, 1C, C$^{4'}$], 125.3 [s, 1C, $^3J_{PtC}$ = 10 Hz, C^5], 126.8 [s, 1C, $^3J_{PtC}$ = 21 Hz,

C^3], 128.99 [s, 2C, $^2J_{PtC}$ = 77 Hz, C^o of *p*-Me-C_6H_4], 131.6 [s, 1C, C^p of *p*-Me-C_6H_4], 133.6 [s, 1C, $^2J_{PtC}$ = 89 Hz, $C^{3'}$], 136.6 [s, 1C, $C^{5'}$], 136.9 [s, 2C, $^3J_{PtC}$ = 25 Hz, C^m of *p*-Me-C_6H_4], 139.3 [s, 1C, C^4], 143.4 [s, 1C, $^1J_{PtC}$ = not resolved, C^i of *p*-Me-C_6H_4], 147.5 [s, 1C, C^6], 151.5 [s, 1C, $^1J_{PtC}$ = 580 Hz, $C^{2'}$], 152.4 [s, 1C, C^2], 158.5 [s, 1C, $C^{1'}$]; δ(^{195}Pt) = -3860.4 [s, Pt].

[Pt(O-bpy)(*p*-Me-C_6H_4)(κ^1-*P*-dppm)], 2a. To a solution of **1** (100 mg, 0.193 mmol) in acetone (10 mL), dppm (75 mg, 0.193 mmol) was added. **1** was gradually solved and reacted with dppm. After 1 hour, the resulting yellowish white precipitate was filtered and washed with *n*-pentane (3×3 mL) and dried under air atmosphere. Yield: 86%; m.p. = decomposed at 268 °C. Elem. Anal. Calcd. for $C_{42}H_{36}N_2OP_2Pt$ (841.77) C, 59.92; H, 4.31; N, 3.33. Found: C, 59.74; H, 4.39; N, 3.37. NMR data in $CDCl_3$: δ(^{1}H) = 2.22 [s, 3H, Me of *p*-Me-C_6H_4], 2.57 [br d, 2H, $^3J_{PH}$ = 9.1 Hz, $^3J_{PtH}$ = 27.3 Hz, CH_2 of dppm], 6.66 [dd, 1H, $^3J_{HH}$ = 7.5 Hz, $^3J_{HH}$ = 5.6 Hz, H^5], 6.77 [d, 2H, $^3J_{HH}$ = 7.6 Hz, H^m of *p*-Me-C_6H_4], 6.93-8.14 [m, 26H, overlapping protons of aromatic rings of *p*-Me-C_6H_4, O-bpy and dppm], 9.92-9.94 [m, 2H, H^3 and H^6]; δ(^{31}P) = 16.7 [d, 1P, $^1J_{PtP}$ = 2216 Hz, $^2J_{PP}$ = 49 Hz, Pt-P], -28.5 [s, 1P, $^3J_{PtP}$ = 54 Hz, $^2J_{PP}$ = 49 Hz, CH_2-P]; δ(^{195}Pt) = -4105.8 [dd, 1Pt, $^1J_{PPt}$ = 2223 Hz, $^3J_{PtP}$ = 56 Hz,].

[Pt_2(O-bpy)$_2$(*p*-Me-C_6H_4)$_2$(μ-dppm)], 2b. To a solution of **1** (100 mg, 0.193 mmol) in acetone (10 mL), dppm (38 mg, 0.97 mmol) was added. **1** was gradually solved and reacted with dppm. After 2 hour, the resulting yellow precipitate was filtered and washed with *n*-pentane (3×3 mL) and dried under air atmosphere. Yield: 79%; m.p. = decomposed at 270 °C. Elem. Anal. Calcd. for $C_{59}H_{50}N_4O_2P_2Pt_2$ (1299.16) C, 54.55; H, 3.88; N, 4.31. Found: C, 54.61; H, 3.94; N, 4.39. NMR data in $CDCl_3$: δ(^{1}H) = 2.25 [s, 6H, Me of *p*-MeC_6H_4], 2.98 [t, 2H, $^3J_{PH}$ = 9.3 Hz, CH_2 of dppm], 6.69-6.77 [m, 8H, $H^{3'}$, $H^{4'}$ and H^m of *p*-MeC_6H_4], 6.88 [dd, 2H, $^3J_{HH}$ = 7.6 Hz, $^3J_{HH}$ = 5.5 Hz, H^5], 6.94 [d, 4H, $^3J_{HH}$ = 7.8 Hz, H^o of *p*-MeC_6H_4], 7.04-7.07 [m, 8H, H^m of dppm], 7.18-7.22 [m, 4H, H^p of dppm], 7.54-7.59 [m, 8H, H^o of dppm], 7.72 [dd, 2H, $^3J_{HH}$ = 5.5 Hz, $^4J_{HH}$ = 1.0 Hz, $^3J_{PtH}$ = 20.7 Hz, H^6], 7.77 [td, 2H, $^3J_{HH}$ = 8.3 Hz, $^4J_{HH}$ = 1.3 Hz, H^4], 8.00 [dd, 2H, $^3J_{HH}$ = 6.5 Hz, $^4J_{HH}$ = 1.0 Hz, $H^{5'}$], 9.87 [d, 2H, $^3J_{HH}$ = 8.4 Hz, H^3]; δ(^{13}C) = 21.0 [s, 2C, Me of *p*-Me-C_6H_4], 53.5 [m, 1C, CH_2 of dppm], 128.4 [s, 4C, $^2J_{PtC}$ = not resolved, C^o of *p*-Me-C_6H_4], 134.2 [s, 4C, $^3J_{PtC}$ = not resolved, C^m of *p*-Me-C_6H_4], 151.3 [s, 2C, $^1J_{PtC}$ = not resolved, $C^{2'}$]; δ(^{31}P) = 15.2 [s, 2P, $^1J_{PtP}$ = 2204 Hz, $^3J_{PtP}$ = 51 Hz, $^2J_{PP}$ = 17 Hz, Pt-P]; δ(^{195}Pt) = -3917.4 [br d, 1Pt, $^1J_{PPt}$ = 2209 Hz].

The synthetic routes for the complexes with sign "**a**" are similar to **2a**, using **1** and one equivalent of corresponding diphosphine ligands. Whilst, the complexes with sign "**b**" are synthesized like **2b** applying **1** and 0.5 equivalent of corresponding diphosphine ligands.

[Pt(O-bpy)(*p*-Me-C$_6$H$_4$)(κ^1-*P*-dppa)], 3a. Yield: 73%; m.p. = decomposed at 239 °C. Elem. Anal. Calcd. for $C_{41}H_{35}N_3OP_2Pt$ (842.19.) C, 58.43; H, 4.19; N, 4.99. Found: C, 57.91; H, 4.67; N, 4.32. NMR data in $CDCl_3$: δ(^{1}H) = 2.26 [s, 3H, Me of *p*-Me-C$_6$H$_4$], 3.89 [br dd, 1H, $^3J_{PH}$ = 14.73, $^3J_{PH}$ = 6.95 Hz, $^3J_{PtH}$ ~ 34 Hz, NH of dppa], 6.70 [dd, 1H, $^3J_{HH}$ = 6.5 Hz, $^3J_{HH}$ = 5.1 Hz, H^5], 6.84-7.91 [m, 28H, overlapping protons of aromatic rings of *p*-Me-C$_6$H$_4$, O-bpy and dppa], 8.01 [d, 1H, $^3J_{HH}$ = 5.1 Hz, H$^{5'}$], 9.94 [d, 1H, $^3J_{HH}$ = 8.2 Hz, H^3]; δ(^{13}C) = 21.1 [s, 1C, Me of *p*-Me-C$_6$H$_4$], 128.2 [d, 2C, $^3J_{PC}$ = 7 Hz, C^o of *p*-Me-C$_6$H$_4$], 128.7 [d, 2C, $^4J_{PC}$ = 1.6 Hz, C^m of *p*-Me-C$_6$H$_4$], 134.4 [s, 1C, $^1J_{PtC}$ = not resolved, C^i of *p*-Me-C$_6$H$_4$], 151.6 [d, 1C, $^1J_{PtC}$ = not resolved, $^2J_{PC}$ = 5 Hz, C$^{2'}$]; δ(^{31}P) = 60.8 [d, 1P, $^1J_{PtP}$ = 2441 Hz, $^2J_{PP}$ = 19 Hz, Pt-P], 28.6 [s, 1P, $^3J_{PtP}$ = 63 Hz, $^2J_{PP}$ = 19 Hz, NH-P]; δ(^{195}Pt) = -4008.7 [dd, 1Pt, $^1J_{PPt}$ = 2472 Hz, $^3J_{PtP}$ = 62 Hz,].

[Pt$_2$(O-bpy)$_2$(*p*-Me-C$_6$H$_4$)$_2$(μ-dppa)], 3b. This complex is mixture product with **3a**. NMR data in $CDCl_3$: δ(^{1}H) = 2.21 [s, 6H, Me of *p*-Me-C$_6$H$_4$], 4.72 [br m, 1H, $^3J_{PtH}$ ~ 23 Hz, NH of dppa], [The aromatic protons of **3b** are considerably overlapped with that of **3a** and cannot be resolved]; δ(^{31}P) = 62.5 [s, 2P, $^1J_{PtP}$ = 2439 Hz, $^3J_{PtP}$ = 45 Hz, $^2J_{PP}$ = 17 Hz, Pt-P].

[Pt(κ^1-*C*-O-bpy)(*p*-Me-C$_6$H$_4$)(dppe)], 4a. Yield: 69%; m.p. = decomposed at 235 °C. Elem. Anal. Calcd. for $C_{43}H_{38}N_2OP_2Pt$ (855.21) C, 60.35; H, 4.48; N, 3.27. Found: C, 60.91; H, 4.51; N, 3.01. NMR data in $CDCl_3$: δ(^{1}H) = 1.84 [m, 4H, CH_2 groups of dppe] 2.05 [s, 3H, Me of *p*-Me-C$_6$H$_4$], 6.67 [d, 2H, $^3J_{HH}$ = 8.6 Hz, H^o of *p*-Me-C$_6$H$_4$], 7.08-7.59 [m, 27H, overlapping protons of aromatic rings of *p*-Me-C$_6$H$_4$, O-bpy and dppe], 7.75 [d, 1H, $^3J_{HH}$ = 6.3 Hz, H$^{5'}$], 8.41 [d, 1H, $^3J_{HH}$ = 4.3 Hz, H^3]; δ(^{31}P) = 38.7 [s, 1P, $^1J_{PtP}$ = 2047 Hz, Pt-P], 41.9 [s, 1P, $^3J_{PtP}$ = 1702 Hz, Pt-P]; δ(^{195}Pt) = -4538.7 [dd, 1Pt, $^1J_{PPt}$ = 2069 Hz, $^1J_{PPt}$ = 1721 Hz].

[Pt$_2$(O-bpy)$_2$(*p*-Me-C$_6$H$_4$)$_2$(μ-dppe)], 4b. Yield: 91%; m.p. = decomposed at 270 °C. Elem. Anal. Calcd. for $C_{60}H_{52}N_4O_2P_2Pt_2$ (1312.29) C, 54.88; H, 3.99; N, 4.27. Found: C, 54.91; H, 4.69; N, 4.31. NMR data in $CDCl_3$: δ(^{1}H) = 1.67 [m, 4H, CH_2 groups of dppe], 2.25 [s, 6H, Me of *p*-Me-C$_6$H$_4$], 6.68-7.89 [m, 46H, overlapping protons of phenyl rings of *p*-Me-C$_6$H$_4$, O-bpy and dppa], 7.98 [d, 2H, $^3J_{HH}$ = 6.3 Hz, H$^{5'}$], 9.90 [d, 2H, $^3J_{HH}$ = 8.3 Hz, H^3]; δ(^{13}C) = 21.2 [s, 2C,

Me of *p*-Me-C_6H_4], 22.9 [m, 2C, CH_2 groups of dppe], 128.9 [d, 4C, $^3J_{PC}$ = 9 Hz, C^o of *p*-Me-C_6H_4], 133.9 [s, 2C, C^p of *p*-Me-C_6H_4], 134.1 [d, 4C, $^4J_{PC}$ = 5 Hz, C^m of *p*-Me-C_6H_4], 151.7 [s, 2C, $^1J_{PtC}$ = not resolved, $C^{2'}$]; δ(^{31}P) = [s, 2P, $^1J_{PtP}$ = 2195 Hz, $^3J_{PtP}$ = 23 Hz, $^2J_{PP}$ = 19 Hz, Pt-P]; δ(^{195}Pt) = -3987.8 [d, 1Pt, $^1J_{PPt}$ = 2249 Hz].

[Pt(κ^1-*C*-O-bpy)(*p*-Me-C_6H_4)(dppp)], 5a. Yield: 71%; m.p. = decomposed at 207 °C. Elem. Anal. Calcd. for $C_{44}H_{40}N_2OP_2Pt$ (869.23) C, 60.76; H, 4.64; N, 3.22. Found: C, 60.14; H, 4.41; N, 3.49. NMR data in $CDCl_3$: δ(^{1}H) = 1.92 [s, 3H, Me of *p*-Me-C_6H_4], 2.51 [br m, 2H, central CH_2 group of dppp], 2.69 [br m, 4H, CH_2 groups adjacent to P of dppp], 6.27 [d, 2H, $^3J_{HH}$ = 6.9 Hz, H^m], 6.50 [d, 2H, $^3J_{PtH}$ = 54.7 Hz, $^3J_{HH}$ = 7.0 Hz, H^o], 6.96-7.83 [m, 27H, overlapping protons of phenyl rings of *p*-Me-C_6H_4, O-bpy and dppp], 8.73 [d, 1H, $^3J_{HH}$ = 4.7 Hz, H^3]; δ(^{31}P) = -4.0 [d, 1P, $^1J_{PtP}$ = 2004 Hz, $^2J_{PP}$ = 23 Hz, Pt-P], -1.8 [d, 1P, $^1J_{PtP}$ = 1673 Hz, $^2J_{PP}$ = 23 Hz, Pt-P]; δ(^{195}Pt) = -4465.9 [dd, 1Pt, $^1J_{PPt}$ = 2014 Hz, $^1J_{PPt}$ = 1675 Hz].

[Pt_2(O-bpy)$_2$(*p*-Me-C_6H_4)$_2$(μ-dppp)], 5b. Yield: 83%; m.p. = decomposed at 192 °C. Elem. Anal. Calcd. for $C_{61}H_{54}N_4O_2P_2Pt_2$ (1326.30) C, 55.20; H, 4.10; N, 4.22. Found: C, 54.91; H, 4.17; N, 4.73. NMR data in $CDCl_3$: δ(^{1}H) = 1.20 [br m, 4H, CH_2 groups adjacent to P of dppp], 1.63 [br m, 2H, central CH_2 group of dppp], 2.21 [s, 6H, Me of *p*-Me-C_6H_4], 6.51 [d, 4H, $^3J_{HH}$ = 7.5 Hz, H^m], 6.68 [d, 4H, $^3J_{PtH}$ = 40.1 Hz, $^3J_{HH}$ = 7.5 Hz, H^o], 6.69-7.96 [m, 39H, overlapping protons of phenyl rings of *p*-Me-C_6H_4, O-bpy and dppp], 8.00 [d, 2H, $^3J_{HH}$ = 6.2 Hz, $H^{5'}$], 9.93 [d, 2H, $^3J_{HH}$ = 7.8 Hz, H^3]; δ(^{13}C) = 19.0 [s, 1C, C-CH_2-C of dppp], 21.0 [s, 2C, Me of *p*-Me-C_6H_4], 27.1 [m, 2C, P-CH_2 groups of dppp], 128.8 [d, 4C, $^3J_{PC}$ = 9 Hz, C^o of *p*-Me-C_6H_4], 133.9 [d, 4C, $^4J_{PC}$ = 6 Hz, C^m of *p*-Me-C_6H_4], 152.1 [s, 2C, $^1J_{PtC}$ = not resolved, $C^{2'}$]; δ(^{31}P) = 19.2 [s, 2P, $^1J_{PtP}$ = 2221 Hz, Pt-P]; δ(^{195}Pt) = -3986.2 [d, 1Pt, $^1J_{PPt}$ = 2252 Hz].

[Pt_2(O-bpy)$_2$(*p*-Me-C_6H_4)$_2$(μ-dppb)], 6b. Yield: 91%; m.p. = decomposed at 223 °C. Elem. Anal. Calcd. for $C_{62}H_{56}N_4O_2P_2Pt_2$ (1340.32) C, 55.52; H, 4.21; N, 4.18. Found: C, 55.73; H, 4.69; N, 3.98. NMR data in $CDCl_3$: δ(^{1}H) = 0.78-1.68 [br m, 8H, CH_2 groups of dppp], 2.03 [s, 6H, Me of *p*-Me-C_6H_4], 6.51 [d, 4H, $^3J_{HH}$ = 7.7 Hz, H^m], 6.91 [d, 4H, $^3J_{PtH}$ = 62.1 Hz, $^3J_{HH}$ = 7.5 Hz, H^o], 6.66-8.01 [m, 38H, overlapping protons of phenyl rings of *p*-Me-C_6H_4, O-bpy and dppp], 9.94 [d, 2H, $^3J_{HH}$ = 8.1 Hz, H^3]; δ(^{31}P) = 20.1 [s, 2P, $^1J_{PtP}$ = 2199 Hz, Pt-P].

[Pt(κ^1-*C*-O-bpy)(*p*-Me-C$_6$H$_4$)(dppbz)], 7a. Yield: 73%; m.p. = decomposed at 183 °C. Elem. Anal. Calcd. for $C_{47}H_{38}N_2OP_2Pt$ (903.21) C, 62.46; H, 4.24; N, 3.10. Found: C, 62.79; H, 4.78; N, 3.27. NMR data in $CDCl_3$: δ(^{1}H) = 2.03 [s, 3H, Me of *p*-Me-C$_6$H$_4$], 6.38-7.71 [m, 42H, overlapping protons of aromatic rings of *p*-Me-C$_6$H$_4$, O-bpy and dppbz], 7.75 [d, 1H, $^3J_{HH}$ = 6.3 Hz, H$^{5'}$], 8.23 [d, 1H, $^3J_{HH}$ = 4.8 Hz, H^3]; δ(^{13}C) = 20.8 [s, 1C, Me of *p*-Me-C$_6$H$_4$], 127.6 [d, 2C, $^2J_{PC}$ = 6.8 Hz, C^o of *p*-Me-C$_6$H$_4$], 147.8 [s, 1C, $^1J_{PtC}$ = not resolved, C$^{2'}$]; δ(^{31}P) = 45.5 [s, 1P, $^1J_{PtP}$ = 2058 Hz, Pt-P], 46.6 [s, 1P, $^3J_{PtP}$ = 1726 Hz, Pt-P]; δ(^{195}Pt) = -4512.1 [dd, 1Pt, $^1J_{PPt}$ = 2048 Hz, $^1J_{PPt}$ = 1722 Hz].

[Pt$_2$(O-bpy)$_2$(*p*-Me-C$_6$H$_4$)$_2$(μ-dppf)], 8b. Yield: 88%; m.p. = decomposed at 261 °C. Elem. Anal. Calcd. for $C_{68}H_{56}N_4O_2P_2FePt_2$ (1468.25) C, 55.59; H, 3.84; N, 3.81. Found: C, 56.01; H, 3.92; N, 3.72. NMR data in $CDCl_3$: δ(^{1}H) = 2.17 [s, 6H, Me of *p*-Me-C$_6$H$_4$], 3.35 [m, 4H, H$^\beta$ of Cp rings], 4.35 [m, 4H, H$^\alpha$ of Cp rings], 6.59 [d, 4H, $^3J_{HH}$ = 6.9 Hz, H^m], 6.96 [d, 4H, $^3J_{PtH}$ = 51.4 Hz, $^3J_{HH}$ = 6.8 Hz, H^o], 7.20-7.86 [m, 30H, overlapping protons of phenyl rings of *p*-Me-C$_6$H$_4$, O-bpy and dppf], 8.03 [m, 2H, H$^{5'}$], 9.92 [m, 2H, H^3]; δ(^{31}P) = 20.2 [s, 2P, $^1J_{PtP}$ = 2205 Hz, Pt-P].

X-ray structure determinations

Single crystals of **1**, **2a**, **2b** and **5b** suitable for X-ray diffraction analysis, were grown by slow layer diffusion of *n*-hexane into dichloromethane solution of the complex. X-ray intensity data for **2a**, **2b** and **5b** were collected using the full sphere routine by φ and ω scans strategy on the Agilent *SuperNova* dual wavelength EoS S2 diffractometer with mirror monochromated Mo *Kα* radiation (λ = 0.71073 Å) for **2b** and Cu *Kα* radiation for **2a** and **5b**. For all data collections except **1**, the crystals were cooled to 150 K using an Oxford diffraction Cryojet low-temperature attachment. The data reduction, including an empirical absorption correction using spherical harmonics, implemented in *SCALE3 ABSPACK* scaling algorithm,[47] was performed using the *CrysAlisPro* software package.[48] The crystal structures of **2a**, **2b** and **5b** were solved by direct methods using the online version of *AutoChem 2.0* in conjunction with *OLEX2* suite of programs implemented in the *CrysAlis* software.[49, 50] Diffraction data for **1** were collected by STOE IPDS 2T diffractometer in a series of ω scans in 1° oscillations and integrated using the STOE X-AREA software package.[51] Numerical absorption correction was applied using X-Red32 software.[52] The structures were refined by full-matrix least-squares (*SHELXL2014-7*) on F^2.[53] The non-hydrogen atoms were refined anisotropically. All of the hydrogen atoms were

positioned geometrically in idealized positions and refined with the riding model approximation, with U_{iso}(H) = 1.2 or 1.5 U_{eq}(C). For the molecular graphics the program SHELXTL was used.[54] All geometric calculations were carried out using the *PLATON* software.[53] Crystallographic data for the structural analysis has been deposited with the Cambridge Crystallographic Data Centre, No. CCDC-1818536 (**1**), CCDC-1818535 (**2a**), CCDC-1818538 (**2b**) and CCDC-1818537 (**5b**). Details of data collection and refinement parameters for **1**, **2a**, **2b** and **5b** are given in Table S1. Selected bond lengths and angles for **1**, **2a**, **2b** and **5b** are listed in Table S2. Details of the hydrogen bonding for for **1**, **2a**, **2b** and **5b** are summarized in Table S3. The crystal structure of **5b** showed the voids content of the solvents which were not easy to model properly. The electron density contribution from the solvent was back Fourier transformed from the whole structure by SQUEZZE routine in PLATON and it was roughly fitted with a molecule of *n*-hexane (76 electron counts).

Results and discussions

Synthesis and Characterization of the Precursor Complex 1

The complex [Pt(O-bpy)(*p*-Me-C_6H_4)(SMe_2)], **1**, (O-bpy = rollover deprotonated 2,2′-bipyridine *N*-oxide) was purely synthesized through the reaction of complex *cis*-[Pt(*p*-Me-C_6H_4)$_2$(SMe_2)$_2$] with 2,2′-bipyridine *N*-oxide under reflux condition (Scheme 2). The obtained complex was characterized employing various one or two dimensional NMR techniques (Figures S1-S8). The ^{1}H NMR spectrum of this complex with full assignments is shown in Figure S1, confirming its successful synthesis. Additionally, the ^{1}H{^{195}Pt} NMR spectrum of **1** clearly indicates the absence of platinum satellites for the signals related to the protons of SMe_2, H^o, H$^{3'}$ and H^6. ^{13}C{^{1}H} NMR spectrum of **1** includes two distinct singlet signals at δ = 20.7 and 21.0 in the aliphatic region which are respectively related to the SMe_2 and Me of *p*-Me-C_6H_4 ligands. However, the aromatic region contains various signals which are accurately assigned in Experimental Section. In this region, one of the most prominent signals appeared as a singlet at δ = 151.5 ppm with large coupling to platinum center ($^1J_{PtC}$ = 580 Hz), being attributed to the C$^{2'}$ of O-bpy. Logically, this signal is absent in the corresponding DEPT 135° spectrum. Similarly, the other signals related to the quaternary carbons (δ = 131.6, 143.4, 152.4 and 158.5 ppm) are absent in the DEPT 135° spectrum. As expected, the ^{195}Pt{^{1}H} NMR spectrum of **1** comprises a clear singlet at δ = -3860.4 ppm.

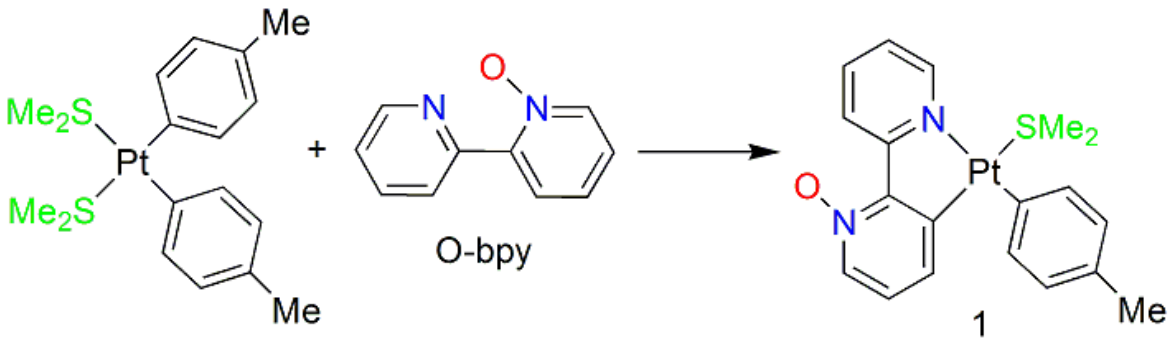

Scheme 2. The route for the synthesis of **1**.

Furthermore, the structure of **1** was further authenticated by X-ray crystallography (Figure 3). The selected bonds and angles for **1** are summarized in Table S2. The appropriate yellow crystals for crystallography were grown by slow layer diffusion of *n*-hexane into the solution of **1** in CH_2Cl_2 solvent. The crystal structure vividly indicates that the O-bpy is located as a C^N-chelated ligand. Also, it can be observed that the *p*-Me-C_6H_4 moiety is located perpendicular in relation to the molecule plane. The crystal packing of **1** shows the formation of centrosymmetric head-to-tail dimer through the intermolecular C–H···O interaction which is supported by π···π interaction with centroid to centroid distances of 3.682(8) and 3.732(7) Å (Figure S9).

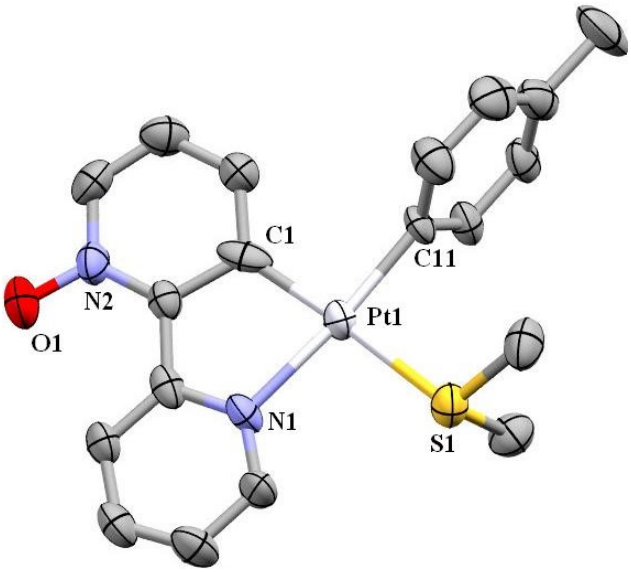

Figure 3. ORTEP plot of **1**. Ellipsoids are drawn at the 40% probability level, and hydrogen atoms are omitted for clarity.

Reactivity of 1 toward various diphosphine ligands

The reactivity of **1** toward a wide range of common diphosphines was evaluated. **1** was reacted with 1 or 0.5 equivalent of dppm (1,1-bis(diphenylphosphino)methane) ligand to give the complexes [Pt(O-bpy)(*p*-Me-C_6H_4)(κ^1-*P*-dppm)], **2a**, or [Pt_2(O-bpy)$_2$(*p*-Me-C_6H_4)$_2$(μ-dppm)], **2b**, respectively (Figure 4). The NMR spectra for **2a** and **2b** are shown in Figures S10-16. In **2a**, the monodentate form (dangling) of dppm is present due to that the stability of the five-membered cyclometalated ring is favored over the four-membered ring in chelating dppm. In this way, the $^{31}P\{^1H\}$ NMR spectrum of **2a** (Figure S11) shows two different signals related to the coordinated and uncoordinated P atoms of dppm ligand with respectively large and small couplings to platinum center. However, for **2b**, the observed signal in $^{31}P\{^1H\}$ NMR spectrum completely reveals the presence of two equivalent phosphorus atoms, exhibiting the bridge pattern between two platinum centers. Besides, ^{195}Pt NMR spectrum of **2a** displayed a doublet of doublets due to coupling with two different P atoms, showing only the larger doublet in the spectrum. However, a doublet signal for **2b** is only observed in its ^{195}Pt NMR spectrum. The observed value of coupling constants for both complexes in ^{195}Pt NMR spectra were close to the obtained value from their $^{31}P\{^1H\}$ NMR spectra.

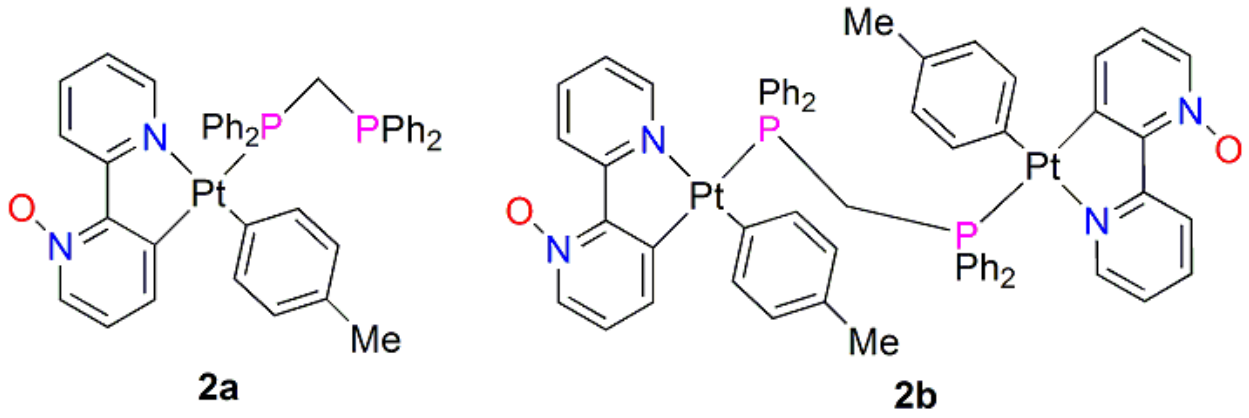

Figure 4. The mononuclear and binuclear cycloplatinated(II) complexes containing dppm ligand.

The structures of **2a** and **2b** have been characterized by X-ray crystallography. Similar to **1**, the suitable single crystals of both complexes were obtained by slow layer diffusion of *n*-hexane into the CH_2Cl_2 solution of the complexes. Figure 5 displays the crystal structures for **2a** and **2b** while the crystal packing views are demonstrated in Figures S17 and S18, respectively.

Also, the selected bond angles for **2a** and **2b** are listed in the Table S2. Crystal structure of **2a** clearly proves dangling form of the dppm ligand. The distance between Pt center and uncoordinated P atom is equal to 4.23 Å which is very close to those reported before.[8] In the binuclear complex **2b**, the Pt centers are not located in front of each other, showing no metal-metal bond between Pt centers. However, in the previously reported cycloplatinated(II) complexes with bridging dppm (containing Me ligand instead of *p*-Me-C_6H_4), intra-molecular Pt-Pt interactions can be observed.[37] For **2b**, the P-C-P angle in dppm ligand was measured to be 129.64° which is larger than that observed for **2a** (112.05°). In **2a**, pair of centrosymmetric C–H···O interactions form dimers which are further connected to one-dimensional extended chain along the a-axis through the intermolecular C–H···N interactions (Figure S17). Also, in **2b**, the intermolecular C–H···O interactions are the main intermolecular interactions which have consolidated the neighboring molecules in the crystal packing (Figure S18).

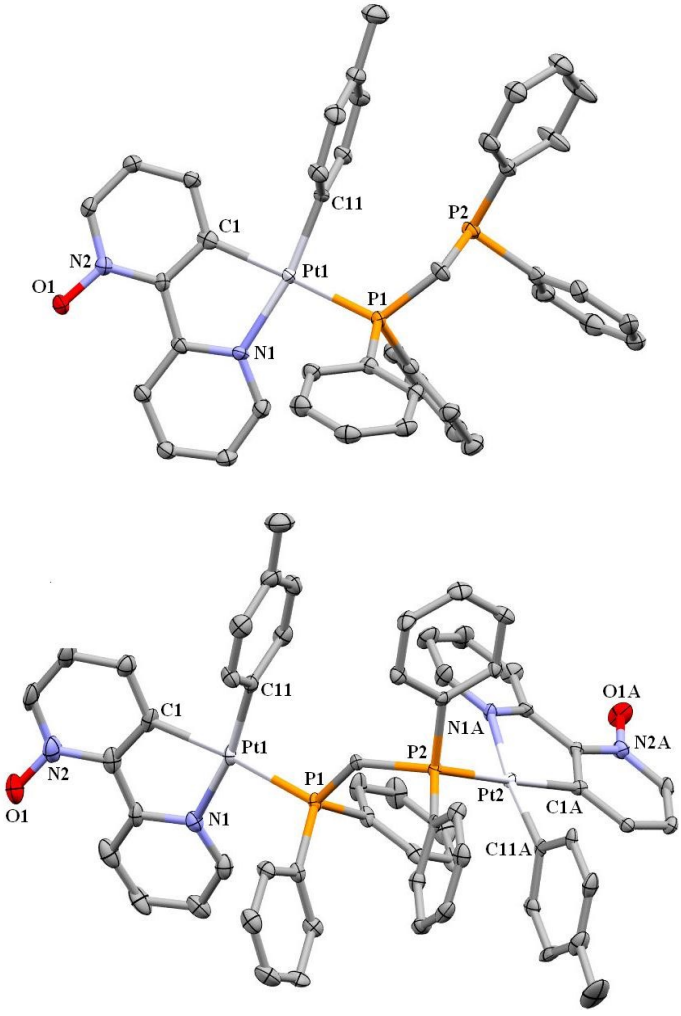

Figure 5. ORTEP plots of **2a** (top) and **2b** (bottom). Ellipsoids are drawn at the 40% probability level. Hydrogen atoms and a CH_2Cl_2 solvent molecule (in **2b**) are omitted for clarity.

The reaction of **1** with 1 equivalent of dppa (N,N-bis(diphenylphosphino)amine) ligand gave the complex [Pt(O-bpy)(*p*-Me-C_6H_4)(κ^1-*P*-dppa)], **3a**, with a dangling dppa ligand (Figure 6). The NMR spectra of **3a** are embedded in the Figures S19-S24. In the ^{1}H NMR spectrum of **3a**, a distinct multiplet signal is observed at δ = 3.89 ppm which is related to the N-H group of the dangling dppa ligand. This signal is converted to a broad singlet signal in the corresponding ^{1}H{^{31}P} NMR spectrum (Figure S20). Interestingly, the signal is vanished in the presence of some amount of D_2O due to that the hydrogen of N-H group can be replaced by deuterium (Figure S21). Similar to **2a**, the ^{31}P{^{1}H} NMR spectrum of **3a**, including two different doublet signals, vividly confirms the presence of monodentate (dangling) dppa. Expectedly, the ^{195}Pt NMR spectrum of **3a** also contains a doublet of doublet signal due to the coupling with two phosphorus atoms of dppa ligand (Figure S24). On the other hand, the reaction of **1** with 0.5 eq of dppa did not proceed to the pure complex [Pt_2(O-bpy)$_2$(*p*-Me-C_6H_4)$_2$(μ-dppa)], **3b**, with bridging dppa ligand (see Figure 6). In addition to the major product of **3b**, both ^{1}H NMR and ^{31}P{^{1}H} NMR spectra exhibit the presence of minor product of **3a** (Figures S25 and S26).

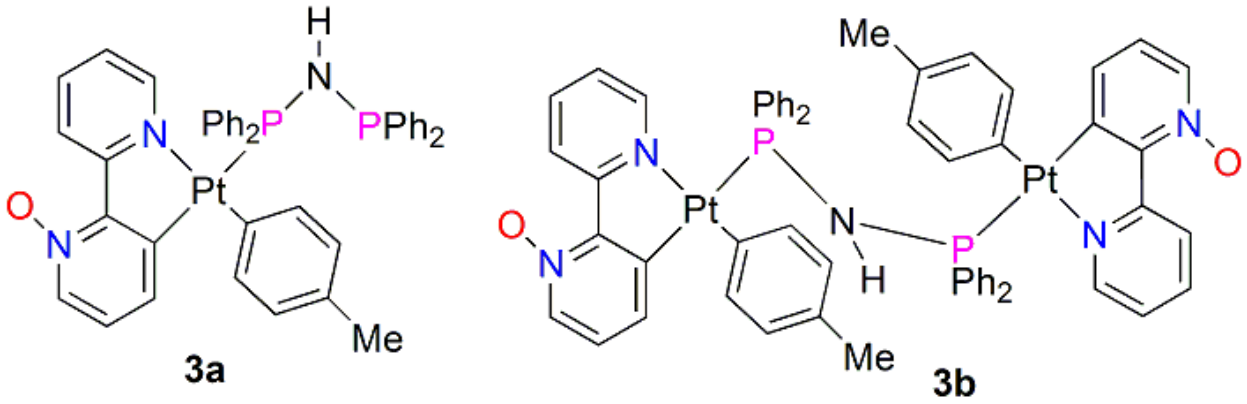

Figure 6. The mononuclear and binuclear cycloplatinated(II) complexes containing dppa ligand.

Dppe (1,2-bis(diphenylphosphino)ethane) and dppp (1,3-bis(diphenylphosphino)propane) ligands contain longer alkyl chains in relation to dppm. They exhibit the same behavior in reaction with **1** (Figure 7). When **1** reacts with 1 equivalent of dppe or dppp, they show a high tendency to make cycloplatinated(II) complexes with chelated diphosphine ligands and yield the complexes [Pt(κ^1-*C*-O-bpy)(*p*-Me-C_6H_4)(dppe)], **4a**, and [Pt(κ^1-*C*-O-bpy)(*p*-Me-C_6H_4)(dppp)],

5a, respectively. Because of high capability of these ligands to coordinate to the central atom as a chelated ligand, the Pt-N bond in cycloplatinated(II) moiety is forced to be broken when chelate is formed. It is expected that, this tendency is higher in dppe in relation to dppp which is due to that dppe is able to form very stable five-membered ring. However, both of them can be located as a bridging ligand between two cyclometalated parts when **1** reacts with 0.5 eq of each ligand and gives the complexes $[Pt_2(O\text{-}bpy)_2(p\text{-}Me\text{-}C_6H_4)_2(\mu\text{-}dppe)]$, **4b**, and $[Pt_2(O\text{-}bpy)_2(p\text{-}Me\text{-}C_6H_4)_2(\mu\text{-}dppp)]$, **5b**. The NMR spectra for **4a**, **4b**, **5a** and **5b** are shown in Figures S27-S40.

The $^{31}P\{^1H\}$ NMR spectra of **4a** and **5a** both contain two different signals flanked with platinum satellites, confirming two different P atoms which are directly connected to platinum center (chelated products). These signals are singlet in the case of dppe (**4a**) showing a very small (not observable) coupling between these two different P atoms, while for **5a** (bearing chelated dppp), both signals appeared as doublet signals. It can be related to the bite angle of chelated diphosphine ligands. Probably, the bite angle for dppp is in such a way that the P atoms can be strongly coupled to each other. Furthermore, the large difference between the chemical shifts arises from the amount of bite angle which is a steric effect imposed by diphosphine backbone. See Figures S28 and S35 for the $^{31}P\{H\}$ NMR spectra of **4a** and **5a**, respectively. Expectedly, ^{195}Pt NMR spectra of both complexes include a doublet of doublet signal due to coupling with two different phosphorus atoms (see Figures S29 and S36 for **4a** and **5a** respectively).

In the case of dimeric complexes with bridging dppe or dppp (**4b** and **5b**), the $^{31}P\{^1H\}$ NMR spectra clearly proves the presence of one signal, presenting two equivalent P atoms. The $^{31}P\{^1H\}$ NMR spectrum of **4b** indicates a signal with splitting pattern related to the "short range-long range" coupling between Pt center and "connected and remote" phosphorus atoms (Figure S32). For **5b**, due to the longer chain of the backbone in dppp compared with dppe, the long range coupling is practically eliminated. Therefore, each phosphine head acts as a monophosphine ligand, making a normal 1:4:1 pattern in the $^{31}P\{^1H\}$ NMR spectrum (Figure S39). As expected, the ^{195}Pt NMR spectra of both **4b** and **5b** have a doublet signal which is due to the coupling of each Pt center with one P atom (Figures S33 and S40).

The appropriate crystals of **5b**, obtained by diffusion of *n*-hexane into its CH_2Cl_2 solution, were further characterized by X-ray crystallography (Figure 8). Similar to the other

crystal structures in this work, *p*-Me-C_6H_4 group is located perpendicular to the molecule plane. The presence of dppp as a bridging ligand is clearly observable. In crystal packing of **5b** the molecules propagated along the [011] direction through C–H···O interactions (Figure S41).

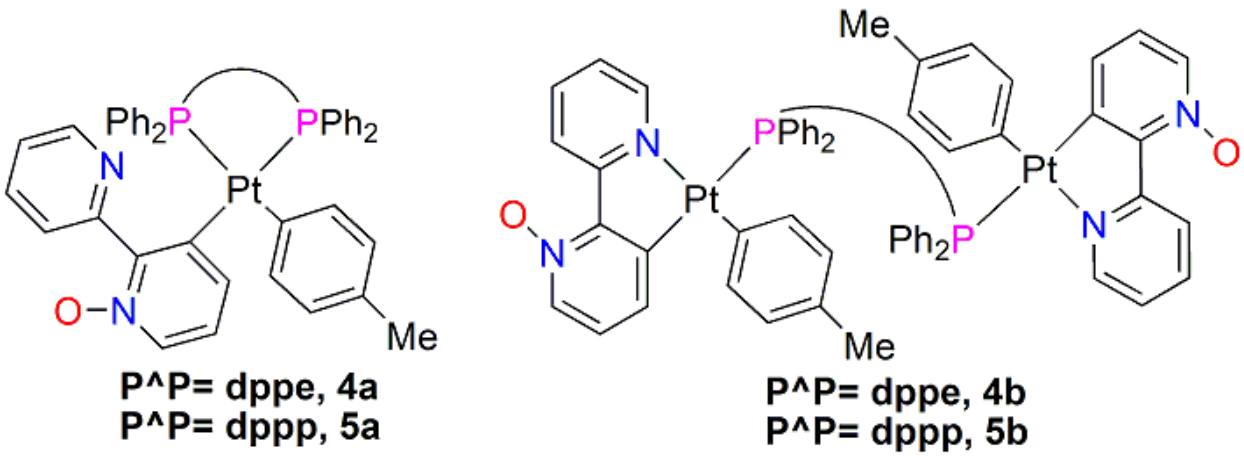

Figure 7. The mononuclear and binuclear cycloplatinated(II) complexes containing dppe or dppp ligand.

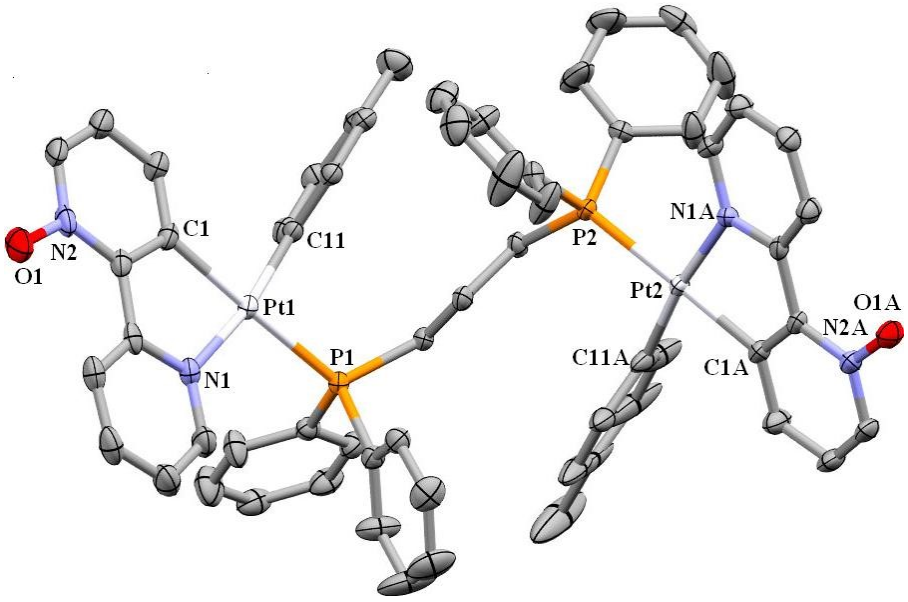

Figure 8. ORTEP plot of **5b**. Ellipsoids are drawn at the 40% probability level, and hydrogen atoms and an *n*-hexane solvent molecule are omitted for clarity.

In order to test the behaviors of dppb (1,4-bis(diphenylphosphino)butane) ligand possessing a longer chain in its backbone relative to dppe and dppp, it was applied in the reaction with **1**. Interestingly, it was observed that dppb ligand is not able to be located as a chelated

ligand. In the reactions with 1:1 and 1:0.5 ratios (**1**: dppb), dppb chose to be a bridging ligand (Figure 9) and produced complex [Pt_2(O-bpy)$_2$(*p*-Me-C_6H_4)$_2$(μ-dppb)], **6b**. In the reaction of **1** with 1 equivalent of dppb, the dimeric product (**6b**) was generated together with 0.5 eq of unreacted free dppb ligand. The unreacted dppb ligand is washed after the reaction terminates. The NMR spectra of **6b** are demonstrated in Figure S42 and S43. Similar to **5b**, the $^{31}P\{^1H\}$ NMR spectrum of the complex **6b** comprises a normal singlet signal with platinum satellites (1:4:1 pattern) because of two equivalent P atoms.

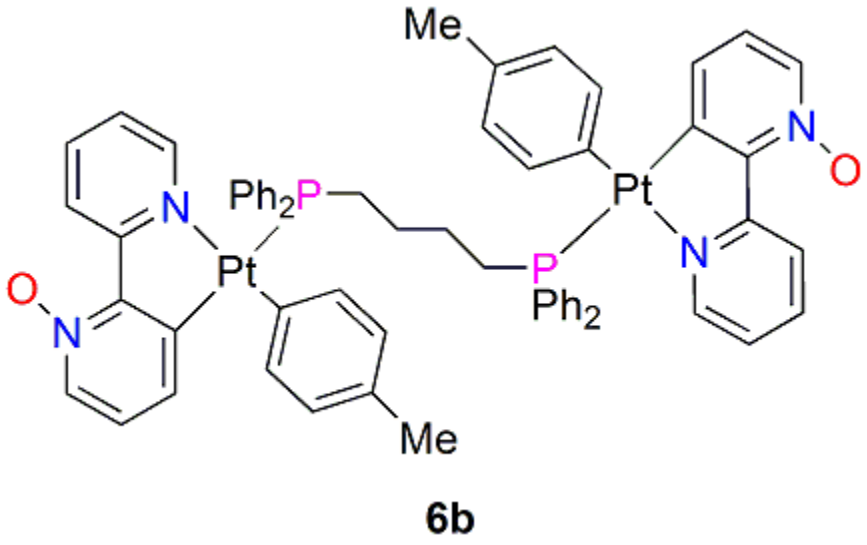

6b

Figure 9. The binuclear cycloplatinated(II) complex containing dppb ligand.

Similar to dppe, dppbz (1,2-bis(diphenylphosphino)benzene) ligand is able to make a five-membered ring in its chelated form. However, the chelation tendency for dppbz is much more intense than dppe so that dppbz cannot be located as a bridging ligand. Definitely, this tendency comes from its rigid backbone (benzene) which effectively hampers the rotation along the bonds between phosphorus atoms. The reaction of **1** with 1 equivalent of dppbz ended up to the formation of complex [Pt(κ^1-*C*-O-bpy)(*p*-Me-C_6H_4)(dppbz)], **7a**, with chelated dppbz ligand. Two different signals with platinum satellites in the $^{31}P\{^1H\}$ NMR spectrum and one doublet of doublet signal in the ^{195}Pt NMR spectrum are the definitive evidences for the structure of **7a**, as shown in Figure 10 (see Figures S46 and S47 for the $^{31}P\{^1H\}$ NMR and ^{195}Pt NMR spectra, respectively). As mentioned above, the dppbz ligand is not able to make a bridge between two cyclometalated fragments so that the reaction of **1** with 0.5 equivalent of dppbz ligand gave **7a**

and half of the unreacted complex **1**. The ^{1}H NMR spectrum for the mixture of **7a** and **1**, shown in Figure S48, clearly confirms the presence of these two components.

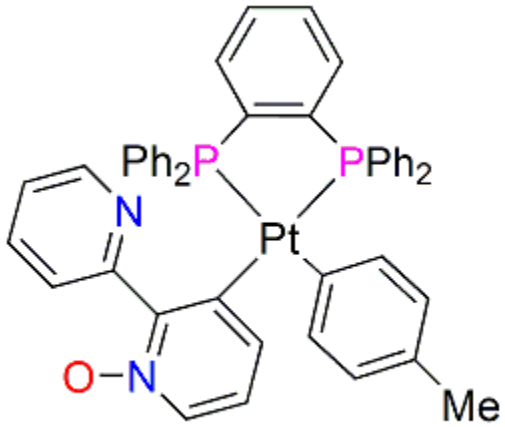

7a

Figure 10. The mononuclear cycloplatinated(II) complex containing dppbz ligand.

Dppf (1,1'-bis(diphenylphosphino)ferrocene) ligand is the last diphosphine ligand which was reacted with **1** in this study. Previously, it has been proved that the reaction of cycloplatinated(II) compounds containing aryl ligands with one equivalent of dppf does not simply proceed like the other diphosphine ligands.[10] Therein, a mechanism was proposed in which the reaction equally results in the formation of two different species; one has chelated dppf and the other one has dangling monodentate dppf. However, these two species are gradually converted to a new species that concurrently includes bridging and dangling dppf.[10] It should be noted that such conversions make the NMR spectra to be very complicated and unexplainable. Interestingly, these conversions do not occur for the cycloplatinated(II) compounds with methyl ligand and their reactions with dppf completely lead to the formation of the pure products with chelated dppf ligand.[20, 55] Conversely, in the reaction of **1** with 0.5 equivalent of dppf, the complex [Pt_2(O-bpy)$_2$(*p*-Me-C_6H_4)$_2$(μ-dppf)], **8b**, is obtained as a pure binuclear complex with the bridging dppf ligand (Figure 11). The NMR spectra of **8b** are shown in Figures S49 and S50. Due to the mentioned reason for the dppp and dppb ligands (**5b** and **6b**), only a singlet signal with platinum satellites is observed in the ^{31}P{^{1}H} NMR spectrum of **8b**, which is indicative of the bridging dppf ligand with two equivalent P atoms.

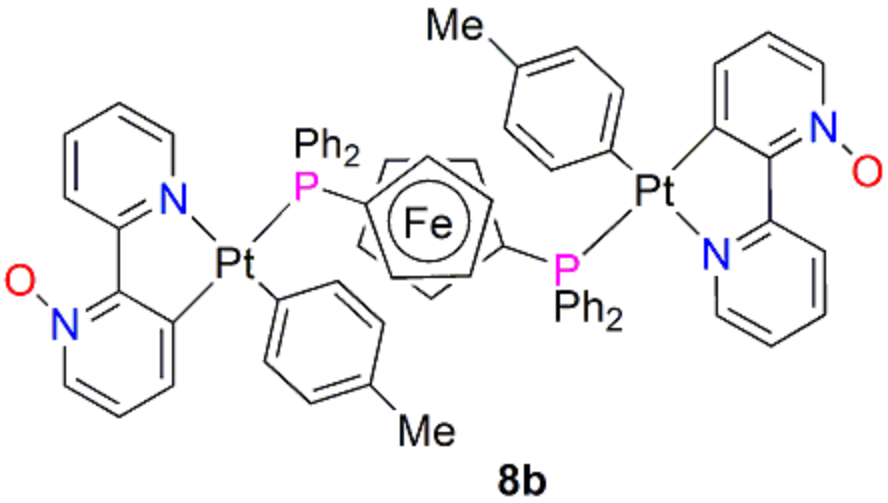

Figure 11. The binuclear cycloplatinated(II) complex containing dppf ligand.

Conclusion

In this work, the reactivity of a new cycloplatinated(II) complex, [Pt(O-bpy)(*p*-Me-C_6H_4)(SMe_2)], **1**, was tested toward a wide range of diphosphine ligands. It was proved that, the diphosphines exhibit various behaviors against **1**, due to their different backbones. All the new complexes were characterized by NMR spectroscopy of the ^{1}H, ^{31}P and ^{195}Pt nuclei. Also, some of them were structurally determined by X-ray crystallography technique.

The reactions of **1** with one equivalent of diphosphines with short backbones (dppm and dppa) yield the products with dangling monodentate diphosphines (**2a** and **3a**). For dppm and dppa, in the first step, SMe_2 is replaced by one phosphine head while the other phosphine head is not able to cleave the cyclometalated Pt-N bond in **1** and consequently remains uncoordinated. In fact, herein, the formation of chelated dppa or dppm with four-membered ring does not have any priority. It is obvious that these two diphosphine ligands can act as bridging ligands when 0.5 equivalent of each is treated with **1**.

In the following, it is observed that dppe and dppp exhibit high tendency to be chelated ligands and make five- and six-membered rings, respectively. As a result, in the reactions with 1:1 ratios (**1**: dppe or dppp), the cyclometalated Pt-N bond is cleaved because of chelation process of the diphosphine. Similar to dppa and dppm cases, they are able to make bridge between two cyclometalated parts in the reactions with 1:0.5 (**1** : dppe or dppp) molar ratios.

Dppb cannot be located as a chelated ligand because of its longer and more flexible backbone (butane) than those of dppe and dppp. Instead, it prefers to be a bridging ligand in both 1:1 and 1:0.5 reactions (**1** : dppb). Conversely, dppbz has a strong tendency (more than dppe) to make five-membered chelated product even in the reaction with 1:0.5 ratio (**1** : dppbz). In dppbz, two PPh_2 moieties are in *ortho* positions relative to each other on a benzene ring. Also, the rigidity of the backbone and formation of five-membered ring are the reasons for the intense tendency of the dppbz to form the chelated products. Finally, dppf proved to be able to make a bridge between two cyclometalated parts in a reaction with 1:0.5 ratio (**1** : dppf). However, as previously reported, the reaction of **1** with 1 equivalent of dppf gives different products.

Electronic supplementary information (ESI) available: NMR spectra and crystallographic data.

Acknowledgments

This work was supported by the Institute for Advanced Studies in Basic Sciences (IASBS) Research Council and the Iran National Science Foundation (Grant no. 95834232). RK is thankful to Sharif University of Technology research Council for the research facility (Grant No. QB960401). RK also thanks Prof. Paul R. Raithby and Bath University for their support. PRR is grateful to the Engineering and Physical Sciences Research Council (EPSRC) for continued funding (EP/K004956/1). Thanks are also due to Mr. A. Biglari, the operator of Bruker NMR instrument at IASBS, for recording the NMR spectra.

References

1. V. De Felice, A. De Renzi, N. Fraldi, G. Roviello and A. Tuzi, *J. Organomet. Chem.*, 2005, **690**, 2035-2043.
2. V. De Delice, A. De Renzi, M. L. Ferrara and A. Panunzi, *J. Organomet. Chem.*, 1996, **513**, 97-104.
3. T. Yagyu, Y. Suzaki and K. Osakada, *Organometallics*, 2002, **21**, 2088-2094.
4. S. M. Nabavizadeh, H. R. Shahsavari, H. Sepehrpour, F. N. Hosseini, S. Jamali and M. Rashidi, *Dalton Trans.*, 2010, **39**, 7800-7805.
5. Y. Suzaki, T. Yagyu, Y. Yamamura, A. Mori and K. Osakada, *Organometallics*, 2002, **21**, 5254-5258.

6. Y. Suzaki and K. Osakada, *Organometallics*, 2004, **23**, 5081-5084.
7. M. Golbon Haghighi, M. Rashidi, S. M. Nabavizadeh, S. Jamali and R. J. Puddephatt, *Dalton Trans.*, 2010, **39**, 11396-11402.
8. S. M. Nabavizadeh, M. Golbon Haghighi, A. R. Esmaeilbeig, F. Raoof, Z. Mandegani, S. Jamali, M. Rashidi and R. J. Puddephatt, *Organometallics*, 2010, **29**, 4893-4899.
9. S. M. Nabavizadeh, H. R. Shahsavari, M. Namdar and M. Rashidi, *J. Organomet. Chem.*, 2011, **696**, 3564-3571.
10. S. M. Nabavizadeh, H. Amini, H. R. Shahsavari, M. Namdar, M. Rashidi, R. Kia, B. Hemmateenejad, M. Nekoeinia, A. Ariafard, F. Niroomand Hosseini, A. Gharavi, A. Khalafi-Nezhad, M. T. Sharbati and F. Panahi, *Organometallics*, 2011, **30**, 1466-1477.
11. A. R. Esmaeilbeig, M. Golbon Haghighi, S. Nikahd, S. Hashemi, M. Mosarezaee, M. Rashidi and S. M. Nabavizadeh, *J. Organomet. Chem.*, 2014, **755**, 93-100.
12. T. Yagyu, J.-i. Ohashi and M. Maeda, *Organometallics*, 2007, **26**, 2383-2391.
13. A. Zucca, A. Doppiu, M. A. Cinellu, S. Stoccoro, G. Minghetti and M. Manassero, *Organometallics*, 2002, **21**, 783-785.
14. B. Butschke and H. Schwarz, *Chem. Sci.*, 2012, **3**, 308-326.
15. J. R. Berenguer, E. Lalinde, M. T. Moreno, S. Sánchez and J. Torroba, *Inorg. Chem.*, 2012, **51**, 11665-11679.
16. J. R. Berenguer, J. Fernández, N. Giménez, E. Lalinde, M. T. Moreno and S. Sánchez, *Organometallics*, 2013, **32**, 3943-3953.
17. J. R. Berenguer, E. Lalinde, A. Martín, M. T. Moreno, S. Ruiz, S. Sánchez and H. R. Shahsavari, *Chem. Commun.*, 2013, **49**, 5067-5069.
18. J. R. Berenguer, E. Lalinde, A. Martín, M. T. Moreno, S. Ruiz, S. Sánchez and H. R. Shahsavari, *Inorg. Chem.*, 2014, **53**, 8770-8785.
19. M. E. Moustafa, P. D. Boyle and R. J. Puddephatt, *Organometallics*, 2014, **33**, 5402-5413.
20. H. R. Shahsavari, M. Fereidoonnezhad, M. Niazi, S. T. Mosavi, S. H. Kazemi, R. Kia, S. Shirkhan, S. Abdollahi Aghdam and P. R. Raithby, *Dalton Trans.*, 2017, **46**, 2013-2022.
21. M. Fereidoonnezhad, M. Niazi, M. Shahmohammadi Beni, S. Mohammadi, Z. Faghih, Z. Faghih and H. R. Shahsavari, *ChemMedChem*, 2017, **12**, 456-465.

22. H. R. Shahsavari, R. Babadi Aghakhanpour, M. Babaghassabha, M. Golbon Haghighi, S. M. Nabavizadeh and B. Notash, *New J. Chem.*, 2017, **41**, 3798-3810.
23. H. R. Shahsavari, R. Babadi Aghakhanpour, M. Babaghasabha, M. Golbon Haghighi, S. M. Nabavizadeh and B. Notash, *Eur. J. Inorg. Chem.*, 2017, 2682–2690.
24. M. Fereidoonnezhad, H. R. Shahsavari, S. Abedanzadeh, B. Behchenari, M. Hossein-Abadi, Z. Faghih and M. H. Beyzavi, *New J. Chem.*, 2018, **42**, 2385-2392.
25. H. R. Shahsavari, R. Babadi Aghakhanpour and M. Fereidoonnezhad, *New J. Chem.*, 2018, **42**, 2564-2573.
26. M. Dadkhah Aseman, S. M. Nabavizadeh, H. R. Shahsavari and M. Rashidi, *RSC Adv.*, 2015, **5**, 22692-22702.
27. M. Jamshidi, S. M. Nabavizadeh, H. R. Shahsavari and M. Rashidi, *RSC Adv.*, 2015, **5**, 57581-57591.
28. M. Niazi and H. R. Shahsavari, *J. Organomet. Chem.*, 2016, **803**, 82-91.
29. M. Niazi and H. R. Shahsavari, *ChemistrySelect*, 2016, **1**, 1780-1783.
30. M. Niazi, H. R. Shahsavari, M. Golbon Haghighi, M. R. Halvagar, S. Hatami and B. Notash, *RSC Adv.*, 2016, **6**, 76463-76472.
31. J. R. Berenguer, E. Lalinde, A. Martín, M. T. Moreno, S. Sanchez and H. R. Shahsavari, *Inorg. Chem.*, 2016, **55**, 7866-7878.
32. M. Niazi, H. R. Shahsavari, M. Golbon Haghighi, M. R. Halvagar, S. Hatami and B. Notash, *RSC Adv.*, 2016, **6**, 95073-95084.
33. M. Golbon Haghighi, S. M. Nabavizadeh, M. Rashidi and M. Kubicki, *Dalton Trans.*, 2013, **42**, 13369-13380.
34. R. Babadi Aghakhanpour, S. M. Nabavizadeh, M. Rashidi and M. Kubicki, *Dalton Trans.*, 2015, **44**, 15829-15842.
35. R. Babadi Aghakhanpour, S. M. Nabavizadeh and M. Rashidi, *J. Organomet. Chem.*, 2016, **819**, 216-227.
36. R. Babadi Aghakhanpour, F. Khoob, A. Shirvanishiri, S. Paziresh, A. R. Esmaeilbeig and A. Wojtczak, *Polyhedron*, 2017, **127**, 17-24.
37. S. Jamali, R. Czerwieniec, R. Kia, Z. Jamshidi and M. Zabel, *Dalton Trans.*, 2011, **40**, 9123-9130.

38. S. M. Nabavizadeh, H. Sepehrpour, R. Kia and A. L. Rheingold, *J. Organomet. Chem.*, 2013, **745–746**, 148-157.
39. H. Samouei, M. Rashidi and F. W. Heinemann, *J. Organomet. Chem.*, 2011, **696**, 3764-3771.
40. S. Fuertes, A. s. J. Chueca and V. Sicilia, *Inorg. Chem.*, 2015, **54**, 9885-9895.
41. L. Maidich, G. Zuri, S. Stoccoro, M. A. Cinellu and A. Zucca, *Dalton Trans.*, 2014, **43**, 14806-14815.
42. F. Zheng, A. T. Hutton, C. G. C. E. van Sittert, W. J. Gerber and S. F. Mapolie, *Dalton Trans.*, 2015, **44**, 1969-1981.
43. J. DePriest, G. Zheng, C. Woods, D. Rillema, N. Mikirova and M. Zandler, *Inorg. Chim. Acta*, 1997, **264**, 287-296.
44. J. DePriest, G. Y. Zheng, N. Goswami, D. M. Eichhorn, C. Woods and D. P. Rillema, *Inorg. Chem.*, 2000, **39**, 1955-1963.
45. B. S. Furniss, A. Hannaford, P. Smith and A. Tatchell, ELBS, 1989.
46. M. Rashidi, M. Hashemi, M. Khorasani-Motlagh and R. J. Puddephatt, *Organometallics*, 2000, **19**, 2751-2755.
47. R. C. Clark and J. S. Reid, *Acta Cryst.*, 1995, **A51**, 887-897.
48. SuperNova Eos S2 System: Empirical absorption correction, 2011, CrysAlis-Software package, Oxford Diffraction Ltd.
49. O. V. Dolomanov, L. J. Bourhis, R. J. Gildea, J. A. K. Howard and H. Puschmann, *J. Appl. Cryst.*, 2009, **42**, 339-341.
50. Agilent (2012): AutoChem 2.0, in conjunction with OLEX2. Agilent Technologies UK Ltd, Yarnton, Oxfordshire, England.
51. Stoe & Cie, X–AREA: Program for the Acquisition and Analysis of Data, Version 1.30; Stoe & Cie GmbH: Darmatadt, Germany, 2005.
52. Stoe & Cie, X–RED: Program for Data Reduction and Absorption Correction, Version 1.28b; Stoe & Cie GmbH: Darmatadt, Germany, 2005.
53. G. Sheldrick, *Acta Cryst.*, 2008, **A64**, 112-122.
54. A. Spek, *Acta Cryst.*, 2009, **D65**, 148-155.
55. S. Jamali, S. M. Nabavizadeh and M. Rashidi, *Inorg. Chem.*, 2008, **47**, 5441-5452.